DOI: 10.1002/cbic.201300708

Hedycaryol Synthase in Complex with Nerolidol Reveals Terpene Cyclase Mechanism

Philipp Baer,[b] Patrick Rabe,[a] Christian A. Citron,[a] Carina C. de Oliveira Mann,[b] Norman Kaufmann,[a] Michael Groll,*[b] and Jeroen S. Dickschat*[a]

The biosynthesis of terpenes is catalysed by class I and II terpene cyclases. Here we present structural data from a class I hedycaryol synthase in complex with nerolidol, serving as a surrogate for the reaction intermediate nerolidyl diphosphate. This prefolded ligand allows mapping of the active site and hence the identification of a key carbonyl oxygen of Val179, a highly conserved helix break (G1/2) and its corresponding helix dipole. Stabilising the carbocation at the substrate's C1 position, these elements act in concert to catalyse the 1,10 ring closure, thereby exclusively generating the anti-Markovnikov product. The delineation of a general mechanistic scaffold was confirmed by site-specific mutations. This work serves as a basis for understanding carbocation chemistry in enzymatic reactions and should contribute to future application of these enzymes in organic synthesis.

Terpenoids represent the largest class of natural products, all deriving from a few linear precursors including geranyl diphosphate (GPP), farnesyl diphosphate (FPP) and geranylgeranyl diphosphate (GGPP).[1] A sophisticated biosynthetic process catalysed by terpene cyclases takes place in order to generate this complexity in chemical space. Despite the existence of structural models for every known class of terpene cyclases,[2] knowledge of the mechanistic principles of the catalysis of terpene biosynthesis is still rudimentary. Here we present crystallographic and functional data for the hedycaryol synthase (HcS) from *Kitasatospora setae*, which converts (2*E*,6*E*)-FPP into (2*Z*,6*E*)-hedycaryol (**1**, Scheme 1). The structure of HcS in complex with nerolidol (**2**, Scheme 1), resembling the intermediate nerolidyl diphosphate (NPP), shows its precisely defined prefolding within the active site and allows for a comprehensive understanding of the enzymatic mechanism. Our results identify 1) the importance of the Val179 carbonyl oxygen and its defined positioning at a helix break motif that is strictly conserved among class I enzymes, 2) the orientation of the helix dipole involved in carbocation stabilisation at the substrate's C1 carbon atom, and 3) the delineation of a general mechanistic scaffold for terpene cyclases that were tested by site-specific mutations. The achieved insights into the terpene cyclases' general mode of action provide a starting point for future work making use of these sophisticated enzymes as tools in organic synthesis.

The KSE_00200t gene of the actinomycete *K. setae* KM-6054 was cloned and expressed in *E. coli*, followed by purification of the protein in its active form. The closest functionally characterised homologue is the caryolan-1-ol synthase from *Streptomyces griseus* (Figure S1 in the Supporting Information).[3–6] The protein was incubated with GPP, (2*E*,6*E*)-FPP, (2*Z*,6*E*)-FPP, (2*E*,6*E*,10*E*)-GGPP and (2*Z*,6*E*)-2-fluorofarnesyl diphosphate (2F-FPP, for synthesis cf. Figure S3), which were synthesised either by literature procedures[7–9] or as shown in Figures S2 and S3. The only accepted substrate was (2*E*,6*E*)-FPP, which was converted at pH 8.5 into (2*Z*,6*E*)-hedycaryol (**1**) and traces of (2*R*,6*E*)-nerolidol (**2**, Figure 1 and Table S1), thus establishing the protein as hedycaryol synthase (HcS). In contrast, incubation at pH 7.0 resulted in **1** and the side products **2**, (2*E*,6*E*)-farnesol (**3**), (*E*)-β-farnesene (**4**) and (3*E*,6*E*)-α-farnesene (**5**).

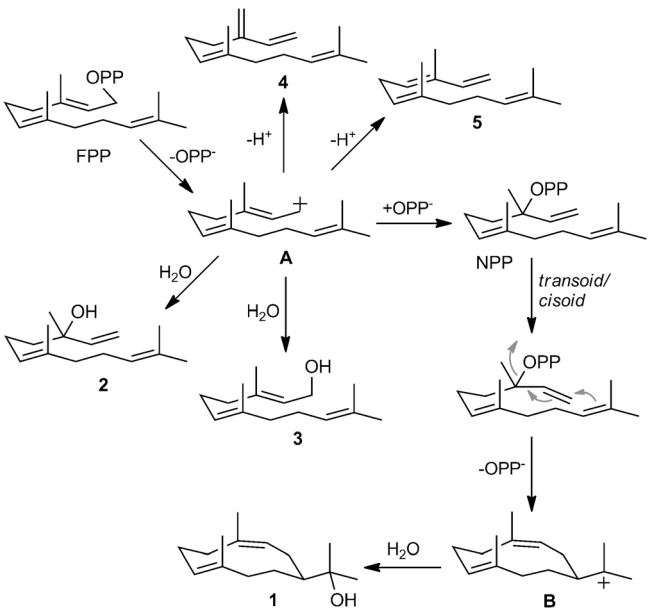

Scheme 1. Cyclisation reactions catalysed by HcS. The scheme shows the cyclisation of FPP to **1** via cationic intermediates, together with all side products.

[a] *P. Rabe,[+] C. A. Citron, N. Kaufmann, Dr. J. S. Dickschat*
Institut für Organische Chemie, Technische Universität Braunschweig
Hagenring 30, 38106 Braunschweig (Germany)
E-mail: j.dickschat@tu-bs.de

[b] *P. Baer,[+] C. C. de Oliveira Mann, Prof. Dr. M. Groll*
Center for Integrated Protein Science at the Department of Chemistry
Lehrstuhl für Biochemie, Technische Universität München
Lichtenbergstrasse 4, 85747 Garching (Germany)
E-mail: michael.groll@ch.tum.de

[+] *These authors contributed equally to this work.*

Supporting information for this article is available on the WWW under http://dx.doi.org/10.1002/cbic.201300708.

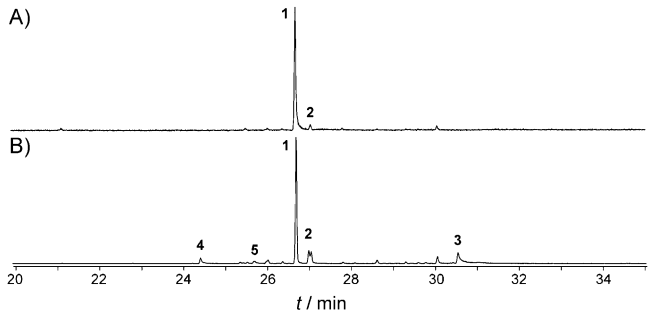

Figure 1. Total ion chromatogram of hexane extracts obtained after incubation of FPP A) with recombinant HcS at pH 8.5, and B) with HcS at pH 7.0. Peak numbers correspond to compound numbers in Scheme 1.

The stability of HcS in the absence and in the presence of the substrate mimetic 2F-FPP was investigated by circular dichroism thermal shift assays (CD-TSAs, Figure S4). The recorded spectra point to a two-step unfolding process. The two-step transition takes place at melting temperatures (T_m) of 41 and 49 °C. On addition of 2F-FPP the two-step unfolding process turns into a one-step transition with an overall T_m of 52 °C; this indicates strong binding to HcS and stabilisation of its thermodynamically distinct structural elements through complexation of this nonreactive substrate analogue in the enzyme's active site.

The conversion of (2*E*,6*E*)-FPP into **1** requires isomerisation to nerolidyl diphosphate (NPP),[10–13] its cyclisation from the *cisoid* conformation and final attack of water (Scheme 1). All side products are formed from intermediate **A** either by quenching with water or by deprotonation. In the main pathway, diphosphate can reattack cation **A** with high efficiency at pH 8.5, whereas its decreased nucleophilicity at pH 7.0 opens up alternative reactions to afford the side products.

HcS belongs to the family of bacterial type I terpene cyclases, a few of which have been crystallised previously.[14–16] In these enzymes the substrate is activated by diphosphate coordination to a trinuclear Mg^{2+} cluster that is bound to two key motifs: the aspartate-rich motif DDxxD and the NSE triad ND-(L,I,V)xSxxxE.[17,18] Diphosphate abstraction generates an allyl cation that eventually cyclises through intramolecular attack(s) of olefinic double bonds at cationic centres, followed by termination either through deprotonation or through attack of water. Insights into catalysis were achieved by determining the crystal structures of apo HcS (2.7 Å, R_{free} = 24.7 %), HcS:HEPES (1.9 Å, R_{free} = 21.9 %) and HcS:**2** (1.5 Å, R_{free} = 18.9 %, Table S2).

Monomeric HcS folds into a single α-domain consisting of 11 antiparallel helices (A–K) that are connected through short loops (Figure S2). The central hydrophobic cavity consists of helices B, C, G, H and K, with helix C containing the highly conserved DDxxD motif and helix H the NSE triad. Both structures lack the Mg^{2+} cluster; this underlines the bidirectional stabilisation of the Mg^{2+} ions and the substrate's diphosphate. Although class I terpene synthases show only little consensus in their primary sequences, the overall tertiary fold is highly conserved.[2,19] A common feature of the class I synthases HcS, pentalenene synthase from *Streptomyces exfoliatus*,[14] epi-isozizaene synthase from *Streptomyces coelicolor*[15] and the α-domain of taxadiene synthase from *Taxus brevifolia*[20] is the previously unrecognised helix break motif G1/2, which positions the carbonyl oxygen atom of a hydrophobic residue (Val179 in HcS) perfectly in line with the G1-helix dipole (Figure 2).

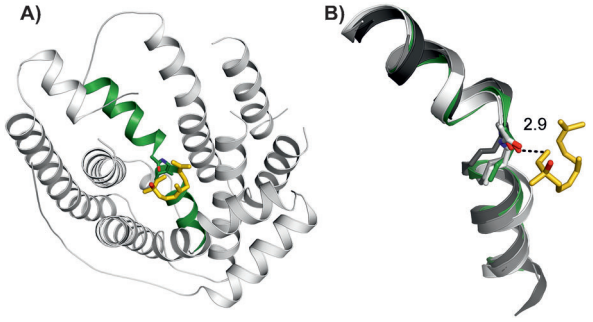

Figure 2. Structure of HcS. A) Ribbon drawing of HcS. The helix G1/2 is shown in green, the Val179 and Gly180 backbones are shown as stick models, nerolidol (**2**) is shown in yellow, oxygen atoms are in red, and nitrogen atoms are in blue. B) Helix G1/2: superposition of HcS (green), pentalenene synthase (grey, PDB ID: 1HM7), epi-isozizaene synthase (dark grey, 3KB9), and taxadiene synthase (light grey, 3P5P). The dashed line indicates the interaction between the carbonyl oxygen atom of Val179 and C1 of **2** (2.9 Å).

Although structures of terpene cyclases bound to unreactive ligands explain initial binding,[16,21] the complex with the reaction intermediate analogue (complex HcS:**2**) at 1.5 Å resolution gives insights into subsequent reaction steps from NPP to **1** and allows for a detailed mechanistic interpretation (Figure 3). The delineated trajectory starts with FPP binding to the Mg^{2+} cluster. As is known from the case of *Aspergillus terreus* aristolochene synthase, this causes a conformational change that closes the active site.[21,22] A rearrangement shifts diphosphate from C1 to C3 to yield NPP. Its presumed folding in the active centre is observed in the HcS:**2** complex, and the short C1–C10 distance in **2** (2.6 Å) perfectly matches the structure of the main product (2*Z*,6*E*)-**1** (Figure 3). NPP cyclisation is initiated by abstraction of diphosphate that is stabilised by the Mg^{2+} cluster and the transient positive charge at C3. The carbonyl oxygen of Val179 and the C-terminal negative helix dipole of G1 are perfectly aligned (2.9 Å) due to the helix break motive and activate the C1 position by shifting the transient carbocation from C3 to C1 (Figure 2; the G1-helix directly points towards C1 of **2**). This supports the nucleophilic attack from the C10/C11 double bond onto C1 to form the anti-Markovnikov product **B** (Scheme 1). The cationic centre at C11 is stabilised by cation–π interaction with the neighbouring Phe149 (Figure 3). This shift of the cation towards C11 causes the release of diphosphate from the active centre, which is no longer stabilised by a charge at C3, followed by collapse of the Mg^{2+} cluster. Asp82 in the ^{82}DDXXD^{86} motif is free now and perfectly oriented (Figure 3) to activate water for the attack at C11 to generate the product **1**.

This suggested mechanism of catalysis was approved by mutagenesis experiments. For this purpose, twelve site-specific

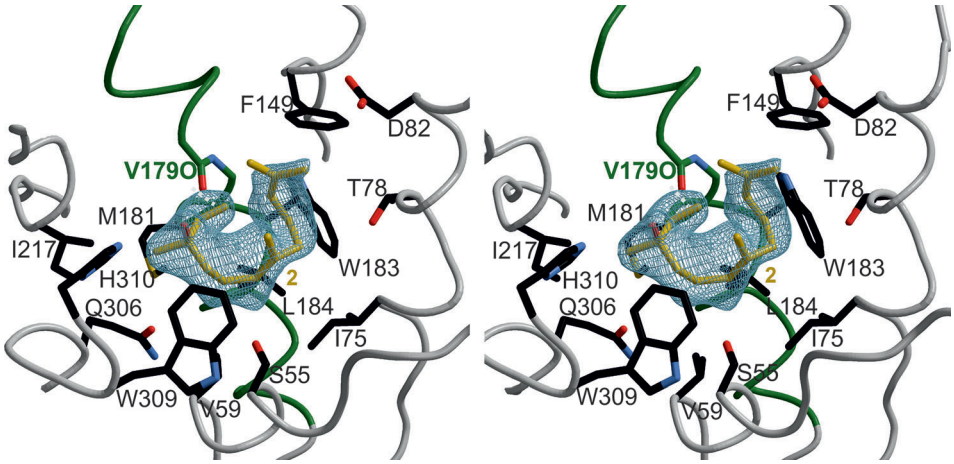

Figure 3. Stereoview of the $2F_o-F_c$ electron density map for the active site of the HcS:**2** complex. Close up view of the catalytic active site of hedycaryol synthase in complex with nerolidol. The orientation and colour coding is as in Figure 2A. Amino acids directly involved in ligand stabilisation are shown in ball-and-stick representation and are labelled. The electron density map is contoured at 1σ and shown in blue; **2** was omitted prior to phase calculations.

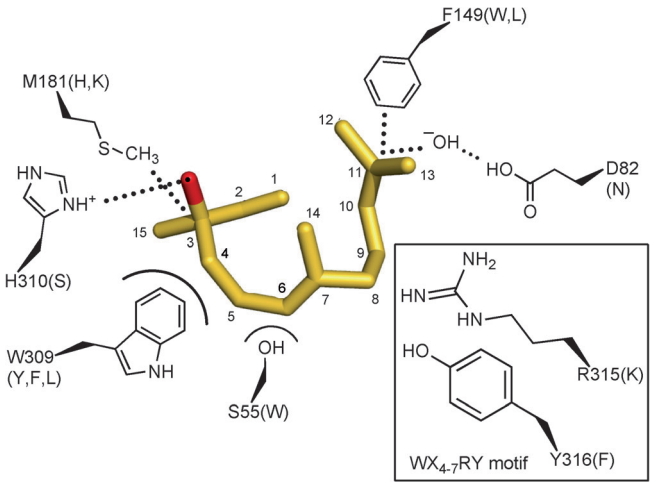

Scheme 2. Summary of the mutagenesis experiments. Nerolidol (**2**), as folded in the active centre of HcS, is shown in yellow. Dashed lines indicate interactions of the residues and the ligand. Arcs indicate unspecific, hydrophobic interactions. Bold residues are functionally relevant as shown in mutation experiments. Boxed amino acids are distant from the active site.

mutants were constructed (Scheme 2 and Table 1). The F149L replacement exhibited strongly decreased production of **1** (Figure S5C), fully consistent with the cation stabilisation at C11 by Phe149. The higher production of **1** at pH 8.5 than at pH 7.0 is explained by the increased nucleophilicity of water. The F149W mutant showed production of **1** similar to the wild type (Figure S5D), thus demonstrating that tryptophan can also act in cation–π stabilisation at C11; this is in line with the recently suggested mechanism for the biosynthesis of 2-methylisoborneol by 2-methylisoborneol synthase.[23] In contrast, involvement of Trp309 in cation–π interactions was ruled out by the mutations W309L, W309F and W309Y, which displayed no significant effects (Figure S6E–G). This is in agreement with an earlier report relating to a W308F mutant of the pentalenene synthase from *S. exfoliatus*.[24] These observations are surprising because Trp309 is found in a highly conserved $WX_{4-7}RY$ motif present in all bacterial sesquiterpene synthase homologues (Table S3), although mutation of this motif (R315K and Y316F) did not alter the enzymatic activity relative to the wild type (Figure S5H and I). These findings might be explained by the fact that the substitutions were executed with functionally conserved residues such as lysine and phenylalanine.

The catalytic involvement of Asp82 in the activation of water, on the other hand, was tested by D82N. At pH 7.0 no production of **1** was observed, whereas at pH 8.5 small amounts of **1** were formed (Figure S5J). These observations rule out a critical role for Asp82 in stabilisation of the Mg^{2+} cluster because it can at least be functionally substituted by Asn. The production of **1** as a function of the pH confirms the importance of water activation by Asp82.

The central Met181 in close proximity to the ligand's C3 (Figure 3) was replaced by basic residues of similar size (M181H and M181K, Figure S5K and L). Histidine appears to exist mainly in the protonated state at pH 7.0, but to a lower degree at pH 8.5, whereas lysine is almost exclusively present in the protonated form at both pH values. A positively charged residue will destabilise the transient charge at C3, and accordingly no production of **1** was observed for the M181K mutant, whereas small amounts of **1** were detected in the case of the M181H mutant. The His310 residue is located in close proximity to Asn221 of the NSE triad and the hydroxy function of **2** (Figure 3). Because of its protonated state this residue presumably assists in diphosphate abstraction, and accordingly no production of **1** was observed for the H310S mutant (Figure S5M). Finally, exchange of Ser55 for a bulky residue in the

Table 1. Site-specific mutants of HcS.

Mutant	Activity[a] pH 7	pH 8.5	Mutant	Activity[a] pH 7	pH 8.5
F149L	inactive	active	F149W	wt	wt
W309L	wt	wt	W309F	wt	wt
W309Y	wt	wt	R315K	wt	wt
Y316F	wt	wt	D82N	inactive	active
M181H	inactive	active	M181K	inactive	inactive
H310S	inactive	inactive	S55W	inactive	inactive

[a] Activities were qualitatively evaluated. wt: activity resembles wild-type activity. "Active": **1** is formed, albeit in significantly lower amounts than by the wild-type enzyme. "Inactive": **1** is not formed.

S55W mutant blocks the active site, and only traces of **1** were observed (Figure S5N).

In summary, the crystal structures of HcS and of HcS in complex with the reaction intermediate surrogate nerolidol (HcS**:2**) were obtained at high resolution. The HcS**:2** complex allowed for a detailed mechanistic interpretation, showing that reionisation of the reaction intermediate NPP is assisted by the carbonyl oxygen of Val179 at a helix break motif. Cationic intermediates are stabilised by a helix dipole and by cation–π interaction with F149, whereas Asp82 of the ^{82}DDXXD^{86} motif is involved in water activation. These and other mechanistic aspects were supported by analysis of twelve site-specific mutants. Future work on the chemical and structural characterisation of terpene cyclases for a deep mechanistic understanding of these sophisticated enzymes is now possible.

Acknowledgements

We thank the staff of PXI of the Paul Scherrer Institute, Swiss Light Source (Villigen, Switzerland) for help with data collection. This work was funded by the Deutsche Forschungsgemeinschaft through an Emmy Noether grant (DI1536/1-3), a Heisenberg grant (DI1536/4-1) and the grant "Duftstoffe aus Actinomyceten" (DI1536/2-1, to J.S.D.), and by the Beilstein Institut zur Förderung der Chemischen Wissenschaften with a scholarship (to P.R.). C.C.O.M. is supported by GRK1721. J.S.D. thanks Stefan Schulz (Braunschweig) for support.

Keywords: biosynthesis · crystal structures · enzyme mechanisms · hedycaryol synthases · terpenes · X-ray diffraction

[1] J. S. Dickschat, *Nat. Prod. Rep.* **2011**, *28*, 1917 – 1936.
[2] E. Oldfield, F.-Y. Lin, *Angew. Chem.* **2012**, *124*, 1150 – 1163; *Angew. Chem. Int. Ed.* **2012**, *51*, 1124 – 1137.
[3] C. Nakano, S. Horinouchi, Y. Ohnishi, *J. Biol. Chem.* **2011**, *286*, 27980 – 27987.
[4] C. A. Citron, J. Gleitzmann, G. Laurenzano, R. Pukall, J. S. Dickschat, *ChemBioChem* **2012**, *13*, 202 – 214.
[5] P. Rabe, J. S. Dickschat, *Angew. Chem.* **2013**, *125*, 1855 – 1857; *Angew. Chem. Int. Ed.* **2013**, *52*, 1810 – 1812.
[6] P. Rabe, C. A. Citron, J. S. Dickschat, *ChemBioChem* **2013**, *14*, 2345 – 2354.
[7] V. J. Davisson, A. B. Woodside, T. R. Neal, K. E. Stremler, M. Muehlbacher, C. D. Poulter, *J. Org. Chem.* **1986**, *51*, 4768 – 4779.
[8] A. B. Woodside, Z. Huang, C. D. Poulter, *Org. Synth.* **1988**, *66*, 211 – 219.
[9] D. J. Miller, F. Yu, R. K. Allemann, *ChemBioChem* **2007**, *8*, 1819 – 1825.
[10] D. Arigoni, *Pure Appl. Chem.* **1975**, *41*, 219 – 245.
[11] D. E. Cane, M. Tandon, P. C. Prabhakaran, *J. Am. Chem. Soc.* **1993**, *115*, 8103 – 8106.
[12] D. E. Cane, M. Tandon, *J. Am. Chem. Soc.* **1995**, *117*, 5602 – 5603.
[13] D. E. Cane, H.-J. Ha, *J. Am. Chem. Soc.* **1986**, *108*, 3097 – 3099.
[14] C. A. Lesburg, G. Zhai, D. E. Cane, D. W. Christianson, *Science* **1997**, *277*, 1820 – 1824.
[15] J. A. Aaron, X. Lin, D. E. Cane, D. W. Christianson, *Biochemistry* **2010**, *49*, 1787 – 1797.
[16] M. Köksal, W. K. W. Chou, D. E. Cane, D. W. Christianson, *Biochemistry* **2012**, *51*, 3011 – 3020.
[17] M. J. Rynkiewicz, D. E. Cane, D. W. Christianson, *Proc. Natl. Acad. Sci. USA* **2001**, *98*, 13543 – 13548.
[18] C. M. Starks, K. Back, J. Chappell, J. P. Noel, *Science* **1997**, *277*, 1815 – 1820.
[19] D. W. Christianson, *Chem. Rev.* **2006**, *106*, 3412 – 3442.
[20] M. Köksal, Y. Jin, R. M. Coates, R. Croteau, D. W. Christianson, *Nature* **2011**, *469*, 116 – 120.
[21] M. Chen, N. Al-lami, M. Janvier, E. L. D'Antonio, J. A. Faraldos, D. E. Cane, R. K. Allemann, D. W. Christianson, *Biochemistry* **2013**, *52*, 5441 – 5453.
[22] E. Y. Shishova, L. Di Costanzo, D. E. Cane, D. W. Christianson, *Biochemistry* **2007**, *46*, 1941 – 1951.
[23] N. L. Brock, S. R. Ravella, S. Schulz, J. S. Dickschat, *Angew. Chem.* **2013**, *125*, 2154 – 2158; *Angew. Chem. Int. Ed.* **2013**, *52*, 2100 – 2104.
[24] M. Seemann, G. Zhai, J.-W. de Kraker, C. M. Paschall, D. W. Christianson, D. E. Cane, *J. Am. Chem. Soc.* **2002**, *124*, 7681 – 7689.

Received: November 12, 2013
Published online on January 7, 2014